

MUTATIONS CONFERRING RESISTANCE TO SCH6, A NOVEL HEPATITIS C VIRUS NS3/4A PROTEASE INHIBITOR: REDUCED RNA REPLICATION FITNESS AND PARTIAL RESCUE BY SECOND-SITE MUTATIONS

†MinKyung Yi^{1,2}, †Xiao Tong⁴, Angela Skelton⁴, Robert Chase⁴, Tong Chen⁴, Andrew Prongay⁵,
Stephane L. Bogen⁶, Anil K. Saksena⁶, F. George Njoroge⁶, Ronald L. Veselenak^{1,3},
Richard B. Pyles^{1,3}, Nigel Bourne^{1,3}, Bruce A. Malcolm⁴ and Stanley M. Lemon^{1,2}

From the ¹Center for Hepatitis Research, Institute for Human Infections & Immunity, and the
Departments of ²Microbiology & Immunology, and ³Pediatrics, University of Texas Medical
Branch, Galveston, TX 77555-1019; ⁴Virology, ⁵Structural Chemistry and ⁶Medicinal Chemistry,
Schering-Plough Research Institute, Kenilworth, NJ 07033.

Running Head: HCV Replication Fitness and NS3/4A Inhibitor Resistance

Address correspondence to: Xiao Tong, Virology, Schering-Plough Research Institute, Kenilworth, NJ 07033, TEL (908) 740-7446; FAX (908) 740-3032; xiao.tong@spcorp.com, or Stanley M. Lemon, University of Texas Medical Branch, Galveston, TX 77555-1019; TEL (409) 747-7048; FAX (409) 747-7030; smlemon@utmb.edu

Drug resistance is a major issue in the development and use of specific antiviral therapies. Here, we report the isolation and characterization of hepatitis C virus (HCV) RNA replicons resistant to a novel ketoamide inhibitor of the NS3/4A protease, SCH6 (originally SCH 446211). Resistant replicon RNAs were generated by G418 selection in the presence of SCH6 in a dose-dependent fashion, with the emergence of resistance reduced at higher SCH6 concentrations. Sequencing demonstrated remarkable consistency in the mutations conferring SCH6 resistance in genotype 1b replicons derived from two different strains of HCV: A156T/V, and R109K. R109K, a novel mutation not reported previously to cause resistance to NS3/4A inhibitors, conferred moderate resistance only to SCH6. Structural analysis indicated that this reflects unique interactions of SCH6 with P'-side residues in the protease active site. In contrast, A156T conferred high level resistance to SCH6 and a related ketoamide, SCH503034, as well as BILN 2061 and VX-950. Unlike

R109K, which had minimal impact on NS3/4A enzymatic function, A156T significantly reduced NS3/4A catalytic efficiency, polyprotein processing and replicon fitness. However, three separate second-site mutations, P89L, Q86R, and G162R, were capable of partially reversing A156T-associated defects in polyprotein processing and/or replicon fitness, without significantly reducing resistance to the protease inhibitor.

Introduction

One of the major issues in development of antiviral drugs is the emergence of drug-resistant virus variants. While antiviral resistance occurs in DNA viruses (1), RNA viruses, such as hepatitis C virus (HCV), have higher mutation rates and typically exist as a complex population of genetically distinct but closely related viral variants, commonly referred to as quasispecies (2-4). During emergence of escape variants, pre-existing minor viral species, resistant to the selecting drug, will gain a growth advantage over

† These authors contributed equally to this work.

the existing wild-type viral population and rapidly become the dominant genotype. In human immunodeficiency virus (HIV)-infected patients treated with protease inhibitors, resistant viruses have been isolated and shown to correlate with relapse of viral replication. Resistance can also be developed by selecting virus with protease inhibitors *in vitro*, and in many cases the mutations that confer resistance *in vitro* are the same as those observed clinically (for review see (5,6)).

Much research has been directed towards finding inhibitors of the non-structural proteins of HCV that contribute to the viral RNA replicase complex. The N-terminal third of NS3 is a serine protease involved in the *cis*-processing of the HCV polyprotein at the NS3-NS4A junction. NS3 assembles as a noncovalent complex with NS4A to form the mature protease responsible for the further processing of the non-structural proteins at the NS4A-NS4B, NS4B-NS5A and NS5A-NS5B junctions (for review see (7)). The NS3 protease is essential for viral replication (8) and represents an important target for antiviral therapy. Recently, a NS3 protease inhibitor, BILN 2061, was reported to reduce viremia by 100-1000 fold in patients during a brief phase Ib clinical trial (9). Another protease inhibitor, VX-950, has also been shown to inhibit HCV replication in pre-clinical studies, and recently was reported to have clinical efficacy similar to that of BILN 2061 (10,11). Mutations conferring resistance to both of these small molecule inhibitors of NS3/4A have been identified in the protease domain by G418 selection of cells containing HCV replicon RNAs expressing neomycin phosphotransferase in the presence of the compounds (10,12,13).

We have studied development of resistance to a novel ketoamide, peptidomimetic protease inhibitor, SCH6 (originally SCH446211). SCH6 specifically inhibits NS3 proteolysis of the viral polyprotein, and also has been demonstrated to reverse the NS3/4A-mediated blockade of double-stranded RNA and virus infection-induced activation of interferon regulatory factor 3 (IRF-3) in cells containing HCV RNA replicons (14,15). We report here the isolation and characterization of SCH6-resistant replicon variants derived from two genotype 1b strains of HCV, and show the

impact of these mutations on the catalytic activity of the protease as well as replicon fitness. We show that mutation of R109 leads to moderate resistance against SCH6, but not other inhibitors of the NS3 protease, reflecting novel interactions of SCH6 with P'-side residues in the protease active site. In contrast, mutation of A156 results in broad resistance against NS3/4A inhibitors from multiple chemical classes, but at a significant cost in terms of catalytic activity and replication fitness. This loss of fitness, however, is partially restored by second-site mutations within NS3.

Experimental Procedures

Control cells and subgenomic HCV replicon lines. The human hepatoma cell line Huh-7 (16) was grown in Dulbecco's minimal essential medium (DMEM) supplemented with 2mM glutamine, non-essential amino acids (NEAA), 10 mM HEPES, 0.075% sodium bicarbonate, 100 U/ml penicillin and 100ug/ml streptomycin, and 10% fetal bovine serum. En5-3 cells, a clonal cell line derived from Huh7 cells by stable transformation with the plasmid pLTR-SEAP (17), were cultured in DMEM supplemented with 10% fetal calf serum, but without NEAA, additional sodium bicarbonate, or HEPES, and with the addition of 2 µg/ml blasticidin (Invitrogen). Cell lines containing HCV replicons were cultured in 0.4-0.5 mg/ml of G418, except for clone 16, for which 1mg/ml G418 was used.

The HCV replicon cell lines used in these studies contained autonomously replicating, selectable dicistronic, subgenomic RNAs (18) derived from two different genotype 1b strains of virus. The Con1 replicon used to select the Huh7-derived cell line, 2H8 1.3, was identical to that described by Lohmann et al. (18), except for the presence of a cell culture-adaptive mutation, S233I, within the NS5A sequence (19). The replicon in the stably selected 2H8 1.3 cell line also contains a spontaneously acquired adaptive mutation, E176G in NS3, as discussed below. We also used an additional replicon cell line for selection of SCH6-resistant mutants, Ntat2ANeo/EG. This was established using En5-3 cells and contains a modified subgenomic replicon derived from the HCV-N strain of HCV that

expresses the human immunodeficiency virus (HIV) tat protein, in addition to neomycin phosphotransferase, from its upstream cistron (17). This replicon also carries the NS3 adaptive mutation E176G. The expression of tat by Ntat2ANeo/EG drives the expression and secretion of secreted alkaline phosphatase (SEAP) in transfected En5-3 cells in a manner that correlates closely with the intracellular abundance of the viral RNA. Thus, measurement of SEAP activity in the supernatant fluids of Ntat2ANeo/EG cells allows real-time estimates of the intracellular abundance of replicon RNA (17,20). For transient replication assays, we used the replicon pNtat2ANeo/EG/SI, which is identical to pNtat2ANeo/EG but also contains the S233I adaptive mutation in NS5A.

Selection of replicons with primary SCH6 resistance mutations and second-site compensatory mutations. To select replicon cell lines resistant to SCH6, replicon-bearing cells ($1-2 \times 10^5$) were plated in a 10-cm dish and cultured with 2.5, 0.5, 0.1 or 0 (2H8 1.3 cells), or 2 or 0 μM SCH6 (Ntat2ANeo/EG cells), in addition to G418. All cells were passed once at a 1:10 ratio once they became confluent. Surviving colonies resistant to both inhibitor and antibiotic were selected and expanded for further analysis.

To select additional mutations that might facilitate replication of the HCV-N A156T mutant (see Results), *in vitro* transcribed RNA (see below) derived from Ntat2ANeo/EG/SI replicon engineered to contain the NS3 A156T mutation was electroporated into En5-3 cells, and cell colonies were selected in the presence of 400 $\mu\text{g/ml}$ of G418. RNA isolated from selected clonal cells was subjected to direct sequencing analysis, as described below.

Evaluation of inhibitor resistance. HCV-N replicons selected for resistance to SCH6 were tested for sensitivity to NS3/4A inhibitors, and the results analyzed, as described previously (20). For the Con1 replicons, cells were seeded at 4000 cells/well in 96-well collagen I-coated Biocoat plates (Becton Dickinson). Twenty-four hrs post-seeding, protease inhibitors were added to replicon cells. The final concentration of DMSO was 0.5%, fetal bovine serum was 5%, and G418

was 500 $\mu\text{g/ml}$. Media and inhibitors were refreshed daily for 3 days, and cells were harvested by lysis in 1x cell lysis buffer (Ambion cat #8721). The replicon RNA abundance was measured by quantitative, multiplex RT-PCR (Taqman) assay with the NS5B PCR primers: 5B.2F, ATGGACAGGCGCCCTGA, and 5B.2R, TTGATGGGCAGCTTGGTTTC, with a FAM-labelled probe, CACGCCATGCGCTGCGG. As with the HCV-N replicons (20), the endogenous control was GAPDH mRNA. The real-time RT-PCR reactions were run on the ABI PRISM 7900HT Sequence Detection System using the following program: 48°C for 30 min, 95°C for 10 min, 40 cycles of 95°C for 15 sec, 60°C for 1 min. The ΔCT values ($\text{CT}_{5\text{B}} - \text{CT}_{\text{GAPDH}}$) were plotted against inhibitor concentration and fitted to the sigmoid dose response model using SAS (SAS Institute Inc.) or PRISM software (Graphpad Software Inc.). IC_{50} was the inhibitor concentration necessary to achieve an increase of 1 in the ΔCT over the projected baseline. IC_{90} was the inhibitor concentration necessary to achieve an increase of 3.2 over the baseline.

Replicon sequence analysis. To identify mutations which conferred resistance to SCH6, total cellular RNA was isolated from selected replicon cells and amplified by RT-PCR as described (21). The RT-PCR products were purified using the QIAquick PCR purification kit (Qiagen) and directly sequenced. Alternatively, replicon cell-derived RT-PCR products were cloned into TOPO TA vector (Invitrogen) and plasmid DNA from multiple bacterial colonies was sequenced. The sequences were aligned using Lasergene software (DNASTAR).

Site-directed mutagenesis. To generate mutant protease expression vectors and mutant replicon constructs carrying individual resistance mutations, nucleotide changes were introduced into plasmid DNA using the QuikChange mutagenesis kit (Stratagene). The parental plasmid expressing His-tagged single chain NS3 protease domain, NS4A₂₁₋₃₂-GSGS-NS3₃₋₁₈₁ (plasmid p24), was described by Taremi et al (22). For mutational analysis of HCV-N replicons in transient replication assays, the parental construct was pNtat2ANeo/EG/SI, identical to pNtat2ANeo/EG but containing the NS5A S233I mutation. All

segments of the cDNA that were manipulated during site-directed mutagenesis were sequenced to confirm the presence of the desired mutation and to exclude adventitious changes.

Evaluation of replicon colony formation efficiency (CFE). 5 μg of each replicon RNA was transfected into 5×10^6 Huh-7 cells in 400 μl of PBS at room temperature. Electroporation conditions were 950 μF and 250 V in a 0.4 cm cuvette using a Gene pulser system (Bio-Rad). Cells were selected with 500 $\mu\text{g}/\text{ml}$ G418 for 2-3 weeks until cell colonies were established. One set of the dishes were stained with crystal violet (from Sigma, 0.48 mg/ml in 3% formaldehyde, 30% ethanol, 0.16 mg/ml NaCl) and the numbers of colonies were recorded. The colony formation efficiency (CFE) was reported as the number of colonies established/ μg of input RNA. Cells from the duplicate set were pooled and expanded for further analysis.

Transient replication assay. RNAs representing the Ntat2ANeo/EG/SI, with and without SCH6 resistance mutations, were synthesized with T7 MEGAScript reagents (Ambion), after linearizing plasmids with *Xba*I. Following treatment with RNase-free DNase to remove template DNA and purification using the RNeasy RNA purification kit (Qiagen), the RNA was transfected into En5-3 cells by electroporation. Briefly, 5 μg RNA was mixed with 2×10^6 cells suspended in 500 μl phosphate buffered saline in a cuvette with a gap width of 0.2 cm (Bio-Rad). Electroporation was with two pulses of current delivered by the Gene Pulser II electroporation device (Bio-Rad), set at 1.5 kV, 25 μF , and maximum resistance. No G418 was added to the media. Transfected cells were transferred to two wells of a 6-well tissue culture plate, and culture medium removed completely every 24 hrs and saved at 4 $^{\circ}\text{C}$ for subsequent SEAP assay. The cells were washed twice with PBS prior to re-feeding with fresh culture medium. Since the culture medium was replaced every 24 hrs in these transient assays, the SEAP activity measured in these fluids reflected the daily production of SEAP by the cells. SEAP activity was measured in 10 μl aliquots of the supernatant culture fluids using the Phospha-Light Chemiluminescent Reporter Assay (Tropix) with the manufacturer's suggested

protocol reduced in scale. The luminescent signal was read using a TD-20/20 Luminometer (Turner Designs, Inc.).

Expression and purification of recombinant mutant proteases. The expression and purification protocol has been described in detail (22). Briefly, plasmid DNAs encoding mutant proteases were transformed into JM109 or BL21 (DE3) cells. Single colonies were used to initiate bacterial cultures in 25 $\mu\text{g}/\text{ml}$ kanamycin at 37 $^{\circ}\text{C}$. When the cell density reached $\text{OD}_{600} \sim 1.5$, the culture was induced with 0.4mM of IPTG and grown at 23 $^{\circ}\text{C}$ for 4 hrs. The cell pellet was resuspended in buffer A (25 mM HEPES, pH 7.3, 300 mM NaCl, 0.1% β -octylglucoside, 10% glycerol, 2 mM β -mercaptoethanol or 0.2 mM DTT), and cells were lysed by passing through a microfluidizer (Microfluids Corp). The lysed supernatants were incubated with Ni-NTA beads (Qiagen) for 2 hrs at 4 $^{\circ}\text{C}$ and then loaded onto columns. The Ni-columns were washed with buffer A supplemented with 20 mM imidazole and 1M NaCl. The bound His-tagged protease was eluted with buffer A supplemented with 250 mM imidazole. The eluted fractions were pooled and dialyzed at 4 $^{\circ}\text{C}$ for 18 hr against 50 mM HEPES, 300 mM NaCl, 5mM DTT, 0.1% β -octylglucoside and 10% glycerol. The purified proteases were analyzed on 4-12% Novex NuPAGE gel (Invitrogen) and aliquoted for storage at -80 $^{\circ}\text{C}$.

Protease activity assay. Recombinant proteases were tested using a chromogenic assay as described by Zhang et al. (23). The assays were performed at 30 $^{\circ}\text{C}$ in 96-well microtiter plates. 100 μl protease was added to 100 μl of assay buffer (25mM MOPS, pH 6.5, 20% glycerol, 0.3M NaCl, 0.05% lauryl maltoside, 5 μM EDTA, 5 μM DTT) containing the chromogenic substrate Ac-DTEDVVP(Nva)-O-4-phenylazo-phenyl ester. The reactions were monitored at an interval of 30 s for 1 hr for change in absorbance at 370 nm using a Spectromax Plus microtiter plate reader (Molecular Devices). To determine the enzyme concentration to be used in the assay, proteases were tested (1.6-100 nM) to achieve $\sim 12\%$ substrate depletion over the course of the assay. To evaluate kinetic parameters of recombinant proteases, a range of substrate concentrations

(0.293-150 μM) was used. Initial velocities were determined using linear regression and kinetic constants were obtained by fitting the data to the Michaelis-Menton equation using PRISM Software. Turnover rates were then calculated based on enzyme concentration (2-9 nM). To assay potency of SCH6 and VX-950, the inhibition constants were determined at fixed concentrations of enzyme (2-9 nM) and substrate (40 μM) and fitted to the two step slow-binding inhibition model: $P = v_s t + (v_0 - v_s)(1 - e^{-kt})/k$ of Morrison and Walsh (24) using SAS. The overall inhibition constant K_i^* ($v_s = V_{\max} S / (K_m(1 + I/K_i^*))$) was used as the measure of inhibitor potency. For BILN 2061, the tight-binding inhibition constant (K_i) was calculated by: $K_i = (I - E(1 - v/v_0)) / (v_0/v - 1)$, as described (25).

NS3/4A protease disruption of interferon regulatory factor 3 (IRF-3) signaling.

Huh7 cells were transfected with vectors expressing the wild-type HCV-N NS3-4A segment, with or without SCH6 resistance mutations, a vector expressing an active-site NS3 mutant containing alanine substitutions at residues 138 and 139 (S138AA), or with empty vector, using FuGENE 6 transfection reagent (Roche Molecular Biochemicals). Twenty-four hrs later, cells were transfected with p561Luc, an interferon-stimulated gene 56 (ISG56) promoter luciferase reporter construct, then infected with Sendai virus approximately 8 hrs later (14,15). Cells were harvested the following day and luciferase activities measured. The promoter stimulation index was calculated as the ratio of luciferase activities present in similarly transfected cells with and without Sendai virus infection.

***In vitro* polyprotein cleavage assays.** *In vitro* transcribed RNA, prepared as described above, was used to program *in vitro* translation reactions in rabbit reticulocyte lysate (Promega). For analysis of the impact of NS3 mutation on the *cis* auto-proteolysis of NS3-4A, 1 μg RNA encoding the NS3-4A sequence was used to program a 50 μl reaction mixture containing 2 μl of [³⁵S]-methionine (1,000 Ci/mmol at 10 mCi/ml) and 1 μl of an amino acid mixture lacking methionine. Translation was carried out at 30 °C. Aliquots were removed from the reaction at 20 min, 30 min and 180 min, and SDS sample buffer

added to stop further processing. Translation products were separated by SDS-PAGE followed by autoradiography or PhosphorImager (Molecular Dynamics) analysis. For analysis of *trans*-cleavage reactions, unlabeled NS3/4A protease was produced in an *in vitro* translation reaction as above, but using non-radioactive amino acids, and allowing translation to continue at 30 °C for 180 min to achieve complete auto-proteolysis of NS3-4A (see Fig. 4). A labeled substrate, representing the NS4B-NS5A segment of the polyprotein, was produced by *in vitro* translation in the presence of [³⁵S]-methionine, in rabbit reticulocyte lysates programmed with the appropriate RNA. The *trans*-cleavage assay was carried out as described by Back *et al.* (26). Briefly, 5 μl of the NS3/4A protease and 1 μl of the NS4B-5A substrate were mixed in 25 μl cleavage buffer (25mM sodium phosphate (pH 7.6), 10mM DTT, and 0.1 %CHAPS). Proteolysis was allowed to proceed at 30 °C for 180 min, and samples analyzed as for the *cis*-cleavage assay described above.

Western blot analysis. Cell lysates were separated on 4-12% Novex NuPAGE gel (Invitrogen) and transferred to a PVDF membrane (Invitrogen). The NS5A antibody (1126) was a monoclonal antibody provided by Dr. Johnson Y. N. Lau and was used at 1:5000. The western blot analysis was carried out using the ECF western blot kit (Amersham Life Science). The blots were scanned using a PhosphorImager and visualized using ImageQuant software (Molecular Dynamics).

Structural analysis and modeling. The crystal structure of the full-length single chain NS3 bifunctional protease-helicase (27) and the co-crystal structure of SCH6 and the NS3 protease domain were used to evaluate the impact of mutations. The X-ray structure of the NS3 protease-SCH6 complex was obtained as previously described (28). Point mutations were modeled into the three-dimensional structures using the InsightII molecular modeling program (Accelrys Software Inc., San Diego, CA.). Details of the structural analysis will be published elsewhere (Prongay *et al.*, in preparation).

Results

Generation of HCV replicon cells resistant to SCH6. SCH6-resistant subgenomic HCV RNA replicons were selected from two stably transduced, G418-resistant cell lines harboring subgenomic, dicistronic, replicon RNAs derived from two different genotype 1b strains of HCV (Table 1). The 2H8 1.3 cell line contains replicon RNA derived from the Con1 strain of HCV, while Ntat2aNeo/EG replicon cells contain RNA derived from the HCV-N strain (17). Both of these RNA replicons encode an E176G substitution near the carboxyl terminus of the NS3 protease domain that has been shown previously to promote the replication of HCV RNA in Huh7 hepatoma cells (29). Interestingly, this cell culture-adaptive mutation was independently selected during the establishment of both of these replicon cell lines. HCV RNA replication was inhibited in both the 2H8 1.3 and Ntat2aNeo/EG cell lines by addition of SCH6 to the culture medium, with IC_{90} values of 0.4 and 1.6 μ M (Table 1), respectively. In contrast, measurements of cellular MTT activity and RT-PCR assays for cellular GAPDH mRNA indicated that the CC_{50} for SCH6 was >10 μ M. Thus, SCH6 selectively inhibits HCV RNA replication and has low toxicity for Huh7 cells.

In preliminary experiments, the 2H8 1.3 cells containing the Con1 replicon were cultured in the presence of 0.1-2.5 μ M of SCH6 with continued G418 antibiotic selection in an effort to force the selection of variant replicons with resistance to the NS3/4A protease inhibitor. A majority of the cells were expected to die due to the loss of antibiotic resistance as a result of inhibition of RNA replication, and the subsequent reduction in replicon copy number and neomycin phosphotransferase expression. Cells that survived were presumed to be able to maintain a minimal level of replication in the presence of the compound, and were evaluated for resistance to the compound. When cells were treated with SCH6 at a concentration equaling the IC_{90} , all of the cells survived. On the other hand, when SCH6 was added to the media at ~ 6 -fold the IC_{90} (2.5 μ M), only 0.1% of the cells survived, suggesting that the compound had achieved near complete inhibition of virus RNA replication. Moreover, subsequent quantitative RT-PCR testing indicated

that there was a ~ 33 -fold increase in the SCH6 IC_{90} value for the surviving cells, suggesting that the surviving cells contained replicon RNAs selected for resistance to the inhibitor.

Identification and characterization of mutations associated with resistance to SCH6.

Using the approach described in the previous section, we selected two independent colonies of 2H8 1.3 replicon cells that were resistant to SCH6. We also selected 3 colonies of SCH6-resistant replicon cells from the HCV-N replicon cell line, Ntat2aNeo/EG. The nucleotide sequences of the NS3 protease domains in each of these 5 SCH6-resistant replicon cell lines were determined by direct sequencing of RT-PCR products and compared with the cognate baseline parental sequences (Table 2). Remarkably, the replicon RNA in each of the two Con1 cell lines and in 2 of the 3 HCV-N cell lines contained an R109K mutation. This was the only mutation identified within the NS3 protease domain of the two HCV-N cell lines, while in each of the Con1 cell lines this mutation was found in association with a second I153V substitution (Table 2). The third SCH6-resistant HCV-N cell line contained no substitutions at either of these residues, but instead contained an A156T substitution (Table 2). Threonine or serine substitutions of the A156 residue, which is broadly conserved across all HCV genotypes, have been reported previously to cause resistance to other small molecule inhibitors of the NS3/4A protease (10,13). In contrast, I153V and R109K are novel mutations that have not been described previously.

In an effort to identify additional mutations that might possibly be associated with SCH6 resistance, RNA was extracted from a pool of 2H8 1.3 cells selected by growth in 2.5 μ M SCH6, and replicon sequences amplified by RT-PCR were molecularly cloned followed by DNA sequencing. Interestingly, 4 of 7 cDNA clones contained the A156T mutation, while R109K was present in two others in association with either I153V or A156V. The remaining cDNA clone contained a solitary I153V substitution. No additional mutations were identified within the protease domain using this approach. Together, these data suggest a remarkable consistency in the selection of mutations associated with SCH6

resistance in replicon RNAs derived from two different genotype 1b viruses.

To better characterize these mutations, the amino acid changes were introduced into a recombinant single-chain form of the wild-type protease domain (genotype 1b HCV-BK strain) (22), and analyzed for their impact on kinetic parameters as well as inhibitor binding. Individually, these mutations did not cause dramatic changes in the catalytic efficiency of the protease. The k_{cat} values were all within the experimental error of the wild-type enzyme with the exception of I153V which had a modest effect (~3 fold) (Table 3). K_m values were also within experimental error except for A156T which resulted in a decrease in substrate binding of approximately 5-fold. Importantly, however, the chromogenic substrate (23) used in these *in vitro* protease assays binds only to the P-side of the active site (30). Thus, any potential impact on protein substrates that also bind to the P'-side, such as the native viral polyprotein substrate, would not be detected in these assays. We addressed this limitation by carrying out polyprotein processing assays which are described below in a subsequent section.

In contrast to the relatively small effect on proteolysis, a significant increase (19-fold) in the SCH6 inhibition constant (K_i^* , see Materials and Methods) was observed for the A156T mutation (K_i^* was 7 nM for the wild-type protease, and 130 for the A156T mutant, Table 3). This is consistent with previous reports that A156 is a major locus for development of resistance to NS3/4A inhibitors (10,13). Low-to-moderate levels of SCH6 resistance (2.7- to 6-fold) were conferred by I153V and R109K, respectively. In contrast, the double mutation R109K+A156T significantly increased K_i^* over the individual mutations, suggesting that the impact of these changes on binding free energy may be additive (*i.e.*, the K_i^* for the double mutant would be the product of the individual K_i^* s). This double mutation also further increased the K_m . On the other hand, the double mutation R109K+I153V significantly decreased k_{cat} (8-fold), but did not give rise to an additional increase in resistance compared with the single mutations in this *in vitro* assay.

To further confirm the impact of these mutations on the inhibition of protease activity by SCH6, selected mutations were introduced into the Con1 and HCV-N replicon backgrounds, and stable G418-resistant replicon cell lines carrying the mutant proteases were established. The susceptibility of the replicon harbored by each cell line to SCH6 was assessed by quantitative RT-PCR assays for replicon RNA abundance. These results correlated well with those from the *in vitro* protease assays (Table 3). The A156T mutation conferred a relatively high level of resistance (18-fold) to SCH6 in the Con1 replicon, whereas the R109K mutation gave rise to only a 3-fold increase in the SCH6 IC_{90} . Mutation I153V, although conferring a low level of resistance in the *in vitro* assay, did not seem to affect SCH6 inhibition in the replicon assay. Similar results were obtained with the R109K and A156T mutations in the HCV-N replicon (Table 3). As in the cell-free protease assay, the two mutations appeared to work cooperatively when both were introduced into the Con1 replicon, as the double mutation R109K+A156T increased the IC_{90} by at least 100-fold. In contrast, the R109K+I153V double mutant did not further reduce replicon susceptibility to SCH6 (Table 3).

Cross-resistance to SCH 503034, BILN 2061 and VX-950. To investigate whether the mutations we identified as causing SCH6 resistance would also confer resistance to other published NS3/4A protease inhibitors, the mutant recombinant single-chain proteases described above (see Table 3) were assayed for their susceptibility to other small molecule inhibitors of NS3/4A, including the related ketoamide SCH 503034, the macrocyclic peptidomimetic BILN 2061, and VX-950. An additional mutant protease was similarly assessed, bearing the D168V mutation which was previously reported to confer resistance to BILN 2061 (10,13). As shown in Table 4, the resistance profiles of these compounds differed from that of SCH6. The rank order of the degree of resistance conferred by the mutations toward SCH6 was A156T > R109K > I153V, whereas the D168V mutation had no impact. On the other hand, for BILN 2061, the rank order was A156T > D168V, while R109K and I153V had no impact. For both SCH 503034 and VX-950, A156T was the only mutation that

caused a significant decrease in potency. Thus, A156T was a major determinant of resistance to all four compounds, but SCH6 remained a relatively potent inhibitor of this mutant protease ($K_i^*=0.13 \mu\text{M}$, compared with K_i^* of 1, 12 and 13 μM for BILN 2061, SCH503034 and VX-950 respectively).

Impact of SCH6 resistance mutations on replicon fitness. The preceding results indicate that the R109K and A156T mutations lead to a loss of SCH6 inhibition of NS3 protease activity. To determine their potential impact on viral replication fitness, two separate approaches were taken. First, we assessed the colony formation efficiency (CFE) of Con1 replicon RNAs bearing these resistance mutations. The number of stable G418-resistant cell colonies obtained per μg of transfected input replicon RNA reflects the efficiency with which the mutant replicon replicates in Huh7 cells and expresses the antibiotic selection marker. As shown in Fig. 1, the R109K mutation had no measurable effect on CFE compared with wild-type RNA, whereas the A156T mutation substantially reduced the number of colonies generated (6% of the wild-type Con1 replicon RNA). The double mutation R109K+A156T demonstrated an even greater reduction in CFE (0.7% of wild-type). These results thus suggested that the impact of these mutations on SCH6 potency was inversely correlated with their effect on replicon fitness.

While the CFE provides an estimate of replication fitness, it does not account for the possible accumulation of additional mutations within the replicon RNA during the colony selection process (19). To more directly measure the impact of the A156T and R109K mutations on replication efficiency, we assessed the amplification of replicon RNA following its transfection into permissive cells in a transient replication assay. This was carried out by introducing the mutations into the subgenomic HCV-N replicon, Ntat2ANeo/EG/SI, which expresses the human immunodeficiency virus (HIV) tat protein as well as neomycin phosphotransferase from the upstream cistron (17). This induces the synthesis and release of secreted alkaline phosphatase (SEAP) from transfected En5-3 cells in which SEAP expression has been

placed under the control of the HIV long terminal repeat promoter. The amount of SEAP expressed correlates closely with the intracellular abundance of the viral RNA (17). This novel reporter function significantly facilitates measurement of the replication of transfected replicon RNA in transient assays in which the emergence of adaptive mutations is unlikely to play a significant role. Wild-type Ntat2ANeo/EG/SI and mutant replicon RNAs bearing either the A156T or R109K mutations were transfected into permissive En5-3 cells in parallel with a control, replication-defective NS5B ΔGDD mutant, and the SEAP activity expressed by the cells was monitored every 24 hrs.

As shown in Fig. 2, each of the RNAs induced comparable levels of SEAP activity during the first 24 hrs following transfection (approximately 100-fold greater than nontransfected cells), reflecting translation of the transfected input RNA. Over the subsequent 72 hrs, SEAP expressed by cells transfected with the ΔGDD mutant returned to baseline, while that induced by the wild-type Ntat2ANeo/EG/SI replicon demonstrated a sustained increase indicative of RNA replication (17). While inducing demonstrably greater SEAP activity than the ΔGDD mutant, the A156T mutant was markedly impaired in SEAP induction and thus RNA replication compared to the parental Ntat2ANeo/EG/SI replicon. In contrast, the R109K mutant was only slightly less efficient in replicating and inducing SEAP expression than the parental Ntat2ANeo/EG/SI replicon. These results thus confirm that the A156T mutation is associated with very impaired replication fitness, consistent with the reduced CFE of replicons bearing this mutation in Fig. 1. Together, these data confirm the findings of Lu et al. (13) who reported recently that the A156T mutation substantially reduced the replication fitness of a luciferase-expressing HCV replicon.

Partial rescue of replicon fitness by second-site mutations. A Q86R mutation within the protease domain of NS3 has been identified previously as one of the adaptive mutations associated with the enhanced replication activity of cell culture-adapted HCV replicons (19). It has also been identified recently in association with

the A156T mutation following selection of replicons with a high concentration of an SCH6-related NS3/4A protease inhibitor, SCH503034 (Tong et. al., manuscript submitted). For this reason, we assessed its effect on NS3 protease activity, SCH6 resistance and HCV replicon fitness alone and in association with the A156T mutation. As shown in Table 3, the Q86R mutation by itself had no effect on enzyme activity, as measured using the chromogenic assay, or sensitivity to SCH6 *in vitro* when introduced into the Con1 background. The SCH6 sensitivity of the double mutant, Q86R+A156T, was comparable or only slightly less than that of the A156T mutant. However, the CFE of a Con1 replicon carrying the double mutation was significantly higher than the replicon containing the single A156T mutation (Fig. 1), suggesting that Q86R may partially rescue the loss in fitness of A156T.

To explore the possibility that second-site mutations within the NS3 protease domain might partially rescue the loss of replication fitness associated with the A156T mutation, and to ascertain the genetic stability of the A156T mutation, additional studies were carried out with the SEAP-expressing HCV-N A156T mutant. Huh7 cells were transfected with the Ntat2ANeo/EG/SI replicon RNA bearing the A156T mutation and selected for G418 resistance in the absence of the protease inhibitor, SCH6. Under these conditions, the A156T mutant replicon could either retain the sequence of the transfected RNA, undergo reversion to the wild-type NS3 sequence in the absence of SCH6 pressure, or possibly develop second-site mutations that rescue the reduced fitness of the A156T mutant. Five stable G418-resistant, SEAP-expressing cell colonies were selected, and the NS3 region of HCV RNA isolated from these replicon cells was amplified by RT-PCR and directly sequenced. Replicons from 3 of the 5 colonies demonstrated no sequence changes within the protease domain, but retained the A156T mutation. This is consistent with the reduced but still appreciable (6% of wild-type) CFE of the A156T Con1 replicon (Fig. 1). However, the protease domain within the replicon RNAs in the other 2 cell clones each contained a single mutation in addition to the A156T substitution

present in the original, transfected RNA. One of these mutations, P89L, was located in close proximity to the Q86R mutation described above, while the other mutation was G162R.

To determine the impact of these second-site mutations on the replication fitness of the A156T HCV-N mutant, the P89L and G162R mutations were introduced as single additional mutations into the A156T replicon. The replication of these two double mutants (A156T+P89L and A156T+G162R) was then studied in the transient SEAP replication assay described above following transfection of synthetic RNA into En5-3 cells. As shown in Fig. 2, the introduction of either the P89L or G162R mutation partially rescued the RNA replication defect caused by the A156T mutation. This effect was most evident 72-96 hrs post-transfection, and resulted in a 2-3 fold increase in SEAP activity. These results thus confirm the capacity of these second-site mutations to enhance the replication fitness of the A156T mutant. Consistent with the results obtained with the Q86R mutation, these second-site mutations were associated with minimal loss of the SCH6 resistance phenotype conferred by the A156T mutation. Fold increases in the SCH6 IC₅₀ and IC₉₀ values of the A156T+P89L mutant were 26 and 10, and for the A156T+G162R mutant, 22 and 11, respectively (see Table 3). These results were also confirmed in SCH6 inhibition studies in the transient replication assay (data not shown).

Disruption of interferon signaling by proteases containing resistance mutations. The NS3/4A protease cleaves at least two critical host cell signaling proteins, the Toll-like receptor 3 adaptor protein, TRIF, and interferon- β promoter stimulator 1 (IPS-1, also known as MAVS or Cardif), thereby disrupting virus activation of interferon regulatory factor 3 (IRF-3), a transcription factor that controls the synthesis of interferon- β and numerous interferon stimulated genes (ISGs), such as ISG-56 (14,15,31,32). Since these signaling pathways appear to control virus replication, it is possible that the reduction in viral fitness that we observed in association with the A156T resistance mutation could be due to impaired NS3/4A-mediated proteolysis of cellular targets involved in the activation of innate intracellular antiviral responses, such as TRIF or

IPS-1. To assess this possibility, we examined the ability of Sendai virus to activate the ISG56 promoter in Huh7 cells ectopically expressing NS3/4A, either with or without the R109K or A156T resistance mutation (Fig. 3). Although more detailed biochemical analyses will be required to fully assess the impact of the resistance mutations on proteolysis of TRIF or IPS-1 by NS3/4A, the results from this experiment demonstrated equivalent disruption of IRF-3 signaling to the ISG56 promoter in cells expressing either the wild-type protease or mutant proteases containing the R109K or A156T mutation. This suggests that the loss of fitness associated with the A156T mutation is unlikely to be due to impaired evasion of host defense signaling pathways.

Impact of primary resistance and second-site NS3 mutations on polyprotein processing. The results of the cell-free biochemical protease assays presented in Table 3 suggest that the A156T mutation causes a few-fold loss of proteolytic function, which correlates with the lower CFE activity (Fig. 1) and reduced fitness of HCV replicons (Fig. 2) containing this mutation. Such changes were minimal or not evident at all with the R109K and I153V mutants. However, the chromogenic substrate (23) used in the *in vitro* protease assays binds only the P-side of the active site (30) and is an ester rather than an amide linkage. Thus, this assay does not fully assess the potential impact of the resistance mutations on protein substrates that require the scission of the more refractory amide linkage and that bind to the P'-side or indeed make contacts with the protease elsewhere, as is likely to be the case with the native viral polyprotein substrate. We therefore determined the impact of the resistance mutations on processing of the viral polyprotein by NS3/4A. As indicated above, the NS3/4A protease has both auto-catalytic, *cis*-cleavage activity at the junction of NS3 and NS4A in the polyprotein, as well as putative *trans*-cleavage activities (33) at the other downstream cleavage sites: NS4A/4B, NS4B/5A and NS5A/5B. To determine the effect of the resistance mutations as well as second-site mutations on both *cis*- and *trans*-cleavage reactions, we expressed relevant segments of the viral polyprotein in cell-free translation reactions

carried out in rabbit reticulocyte lysate. In both cases, we compared polyprotein processing with that directed by an active site NS3 protease mutant in which S138 and S139 were both substituted with alanine (S138AA mutant).

To assess *cis*-processing, we programmed reticulocyte lysate with RNA encoding the NS3-4A segment of the HCV-N polyprotein, and allowed translation to proceed in the presence of [³⁵S]-methionine. We monitored the efficiency of auto-catalytic processing of the translation product by assessing the amount of NS3 generated at 20, 30 and 180 min (Fig. 4A). Approximately 70% of the wild-type NS3-4A product was processed within 20 min (Fig. 4B and 4C). In contrast, the NS3-4A segment in which the A156T mutation had been introduced underwent less than 25% processing over a similar period of time, although it was nearly completely processed by 180 min (Fig. 4C). This result clearly indicates that the A156T mutation renders the NS3-4A segment defective in *cis* auto-processing. Interestingly, consistent with its lesser impact on replication fitness (Fig. 2), the R109K mutation had no detectable impact on *cis*-cleavage activity (Fig. 4B and 4C).

To determine the impact of these mutations on *trans*-cleavage activity, we synthesized the NS3-4A segment in similarly programmed reticulocyte lysate in the absence of [³⁵S]-methionine, and then allowed auto-catalytic processing to proceed over a period of 3 hrs. As shown in Fig. 4B and 4C, each mutant achieves greater than 95% *cis*-cleavage by this point in time. We then added these unlabelled, mature enzymes to a labeled substrate comprising the NS4B-5A polyprotein segment that was also expressed in reticulocyte lysates in the presence of [³⁵S]-methionine (see Materials and Methods). We determined *trans*-cleavage activity by assessing the amount of mature NS4B product produced over time (Fig. 5). Compared to the wild-type NS3/4A protease, the A156T mutant showed markedly decreased *trans*-cleavage activity while the R109K mutant was not significantly different from the wild-type with respect to its ability to process the NS4B-5A substrate (Fig. 5B and 5C).

Polyprotein processing, particularly auto-proteolysis at the NS3-4A junction, may be rate limiting in viral RNA replication (33). Thus, we considered it possible that the partial rescue of replicon fitness conferred by the second-site P89L and G162R mutations might be associated with similar restoration of these A156T-associated defects in polyprotein processing. Analysis of the *cis* auto-proteolysis activity of double mutants demonstrated that both the G162R and P89L mutations partially restored the *cis*-processing defect conferred by A156T (Fig. 4). While the P89L mutation partially corrected the *trans*-cleavage defect caused by A156T mutation, the G162R mutation had no effect on this defect (Fig. 5). Interestingly, the P89L mutation was more effective than the G162R mutation in restoring the A156T defect in both the *cis*- and *trans*-cleavage assays (Figs. 4 and 5), despite the fact that both mutations restored RNA replication fitness to comparable degrees (Fig. 2).

To further investigate the effect of these mutations on NS3/4A protease activity in the context of HCV RNA replication, we determined their impact on the efficiency of polyprotein processing in Con1 replicon cells bearing SCH6 resistance mutations. Consistent with the lower catalytic efficiency of the mutant proteases (Table 3) and the results of studies with *in vitro* translation products presented above (Figs 4. and 5), immunoblots using antibody to NS5A demonstrated a processing intermediate (p110) in replicon cells bearing the A156T and A56T+R109K mutations, but not in cells harboring the wt replicon (Fig. 6, compare lane 2 with 5 and 7). This polypeptide is likely the uncleaved product of NS5A-5B based on its size and reactivity with both NS5A and NS5B antibodies (Tong et. al., unpublished data). Compared with the single A156T mutant, the amount of the p110 processing intermediate was reduced in the A156T+Q86R mutant (Fig. 6, lane 6), consistent with a compensatory effect of this second-site mutation on proteolytic function. These results suggest that processing of the polyprotein is near rate-limiting in HCV replication; a few-fold decrease in proteolysis would therefore be expected to lead to a significant loss in fitness. Taken in aggregate, the results presented above indicate that the A156T

mutation causes a loss of fitness in RNA replication that is associated with an impairment in both *cis*- and *trans*-processing of the polyprotein. Second-site mutations that partially restore replication fitness also improve the efficiency of polyprotein processing.

Discussion

Development of drug resistance is a major cause for failure of antiviral therapy. Recent studies on HCV protease inhibitors suggest that variants resistant to drug treatment are readily generated using subgenomic replicon systems (10,12,13)]. In this study, resistance mutations in the HCV protease domain were generated by culturing replicon cells in the presence of a novel protease inhibitor, SCH6, with continued G418 selection. Consistent with previous reports studying other NS3/4A inhibitors, we found that an A156T mutation conferred high level resistance to SCH6 (>14-18 fold) (Table 3). However, two novel mutations were also identified, I153V and R109K, that have not been reported previously in studies of NS3/4A inhibitor resistance. These were found to confer very low to moderate levels of resistance to SCH6 (<4 fold). We found a remarkable consistency in the resistance mutations selected in studies utilizing replicon RNAs derived from two, quite distinct genotype 1b viruses, Con-1 and HCV-N. Certain combinations of the mutations (R109K+A156T, R109K+I153V) were also identified after selection with SCH6. Additional studies demonstrated that the double mutant, A156T+R109K, had substantially increased resistance to SCH6, reflecting the sum of the impact of each mutation on binding of the substrate, and resulting in a multiplicative loss in the activity of SCH6.

Each of the three amino acid substitutions we identified required only a single nucleotide mutation. The baseline prevalence of these resistance mutations in natural HCV isolates may be important in predicting treatment outcome in the clinic. A156 and R109 are 100% conserved in approximately 250 HCV isolates analyzed, whereas significant polymorphism occurs at residue 153, with I153, L153, and V153 found in approximately 74%, 17% and 9% of the sequences in the database, respectively (Ping Qiu, personal

communication). These data may underestimate the true extent of amino acid variation at each of these residues, as minor quasispecies are likely to be underrepresented in the database. Although the degree of SCH6 resistance conferred by I153V is low, and clearly demonstrated only in the cell-free protease assay (Table 3), the natural variation at this position raises the issue of potential differences in treatment responses based on patient isolates.

Although speculative, the cross-resistance studies we carried out using different inhibitor compounds suggest that SCH6 could be advantageous over two previously reported candidate HCV protease inhibitors, BILN 2061 and VX-950, in terms of the emergence of inhibitor resistance (Table 4). Mutation A156T drastically decreased binding of BILN 2061 and VX-950, raising the binding constants to the micromolar range (0.9 and 13 μM respectively), whereas SCH6 remained relatively active ($K_i^*=0.16 \mu\text{M}$). SCH6 was also not affected by a D168V substitution, which confers high level resistance to BILN 2061 (13). Independent of the pharmacodynamic properties of these inhibitors, such differences in the resistance profiles conferred by these mutations could be important considerations in designing future therapeutic regimens. Importantly, our results indicate that higher concentrations of SCH6, which result in more complete suppression of viral replication, significantly decrease the frequency of emergent colonies. Therefore therapies designed to maximally suppress viral replication immediately should help to minimize emergence of resistant populations.

As has been shown in resistance studies of HIV protease inhibitors (34), most of the amino acid residues involved in HCV protease resistance are highly conserved, suggesting that the substitution of these residues may adversely affect protease activity and reduce viral replicative capacity. Indeed, A156T significantly reduced replicon fitness in the CFE assay (6% of wild-type), although R109K by itself had no effect on CFE of the Con1 replicon RNA (Fig. 1). These results are consistent with the results of transient replication assays using the HCV-N replicons, which demonstrated a substantial reduction in the

fitness of the A156T mutant, but little loss of replication fitness with R109K (Fig. 2). Interestingly, the double mutant R109K+A156T demonstrated a greater loss of fitness than the single A156T mutant, as measured in the colony formation assay (0.7% of wild-type) (Fig. 1). Consistent with the loss of fitness imparted by the single A156T mutant, we also documented a decrease in protease enzymatic activity *in vitro* (Table 3 and Figs. 4 and 5), and in mutant replicon cells as evidenced by the accumulation of a polyprotein processing intermediate (Fig. 6). A similar correlation between fitness and enzymatic activity has been reported for HIV protease inhibitors. Certain mutations in the HIV protease domain have been shown to confer high levels of resistance with concomitant decrease in enzyme activity and viral fitness (35-37). Processing intermediates were also observed during infection by mutant viruses in those studies.

Modeling of the mutations into co-crystal structures of the NS3 protease domain with SCH6, BILN 2061 and VX-950 (Prongay et al., *in preparation*) (Fig. 7) provides a logical rationale for the observed cross-resistance or lack thereof. Due to the anti-parallel binding of the three inhibitors, all make close contact with residue 156. The substitution of A156 with residues carrying a larger side chain such as threonine would sterically interfere with inhibitor binding in all cases. I153, although part of the P1-P3 pocket, interacts to varying extents with the three inhibitors. The mutation to valine may weaken enzyme interaction with SCH6, but not with BILN 2061 or VX-950, if less of their binding is dependent on this interaction. A novel feature of SCH6 is that it extends substantially toward the P' side of the active site (Fig. 7B). The phenyl glycine at P'2 appears to interact with residue R109. This interaction would be lost by mutation to lysine, consistent with the resistance of R109K mutants to SCH6 that we identified in this study. This feature is critical to understanding the differences in resistance profiles of the various inhibitors studied in this report. SCH503034, BILN2061 and VX-950 do not interact with this residue, and are therefore not affected by the R109K mutation. While the activities of all three compounds are severely impacted by the A156T mutation on the P side of the active site, SCH6

alone derives a significant part of its binding energy from contacts on both P and P' sides. Mutation of A156 (P side) or R109 (P' side) weakens but does not abolish SCH6 binding. The A156T+R109K double mutation severely impacts SCH6 activity, but requires two mutational events and results in extremely poor replication fitness.

The partial rescue of the mutant A156T replicon by Q86R, P89L, or G162R (Table 3 and Figs. 2, 4 and 5) suggests that, as seen with highly resistant HIV strains, compensatory second-site mutations may arise in HCV mutants that are resistant to protease inhibitors. The fact that Q86R has been observed in replicons without selection suggests that it might offer a growth advantage to replicons in general. However, in addition to enhancing replication fitness, Q86R, like the other compensatory mutations we identified, partially rescues the processing defect that is evident in the A156T mutant. The P89L and G162R mutations both improved *cis* auto-proteolysis at the NS3/4A junction (Fig. 4), while P89L also improved the *trans*-processing activity of the A156T mutant significantly (Fig. 5). In addition, in the presence of the Q86R mutation, the aberrant p110 processing intermediate observed in the A156T mutant Con1 replicon cells was reduced in

abundance, compared to replicon cells with A156T alone or A156T+R109K (Fig. 6). The lack of an impact of these mutations in the biochemical assay (Table 3) may simply reflect the nature of the substrate: a peptide ester binding almost exclusively to the P-side of the active site. The *in vitro* translation/proteolysis studies we carried out are more likely to reflect accurately the impact of the mutations on proteolysis, given the much larger size of the substrates and the potential for interactions with the protease outside of the active site.

Acknowledgements

We thank Drs. Srikanth Venkatraman and Francisco Velazquez, Schering-Plough Research Institute, Kenilworth, NJ, for providing BILN 2061, and VX-950, respectively, and Jeremy Yates, UTMB Galveston, for excellent technical support. This work was supported in part by grants U19-AI40035 (SML) and R21-AI063451 (MY) from the National Institute of Allergy and Infectious Diseases, National Institutes of Health; 004952-0027-2001 (SML) from the Advanced Technology Program of the Texas Higher Education Coordinating Board; and by contract N01-AI25488 (NB) with the National Institute of Allergy and Infectious Diseases.

References

1. Crumpacker, C. (2001) in *Fields Virology* (Knipe, D. M., and Howley, P. M., eds), pp. 393-433, Lippincott Williams & Wilkins
2. Martell, M., Esteban, J. I., Quer, J., Genesca, J., Weiner, A., Esteban, R., Guardia, J., and Gomez, J. (1992) *J Virol* **66**, 3225-3229.
3. Farci, P., Strazzer, R., Alter, H. J., Farci, S., Degioannis, D., Coiana, A., Peddis, G., Usai, F., Serra, G., Chessa, L., Diaz, G., Balestrieri, A., and Purcell, R. H. (2002) *Proc Natl Acad Sci U S A* **99**, 3081-3086.
4. Cabot, B., Martell, M., Esteban, J. I., Piron, M., Otero, T., Esteban, R., Guardia, J., and Gomez, J. (2001) *J Virol* **75**, 12005-12013.
5. Johnson, V. A., Brun-Vezinet, F., Clotet, B., Conway, B., D'Aquila, R. T., Demeter, L. M., Kuritzkes, D. R., Pillay, D., Schapiro, J. M., Telenti, A., and Richman, D. D. (2004) *Top HIV Med* **12**, 119-124
6. Yusa, K., and Harada, S. (2004) *Curr Pharm Des* **10**, 4055-4064
7. Reed, K. E., and Rice, C. M. (2000) in *Current topics in microbiology and immunology: The Hepatitis C viruses* (Hagedorn, C. H., and Rice, C. M., eds) Vol. 242, pp. 55-84, Springer, Heidelberg
8. Kolykhalov, A. A., Mihalik, K., Feinstone, S. M., and Rice, C. M. (2000) *J Virol* **74**, 2046-2051.

9. Lamarre, D., Anderson, P. C., Bailey, M., Beaulieu, P., Bolger, G., Bonneau, P., Bos, M., Cameron, D. R., Cartier, M., Cordingley, M. G., Faucher, A. M., Goudreau, N., Kawai, S. H., Kukulj, G., Lagace, L., LaPlante, S. R., Narjes, H., Poupert, M. A., Rancourt, J., Sentjens, R. E., St George, R., Simoneau, B., Steinmann, G., Thibeault, D., Tsantrizos, Y. S., Weldon, S. M., Yong, C. L., and Llinas-Brunet, M. (2003) *Nature* **426**, 186-189
10. Lin, C., Lin, K., Luong, Y. P., Rao, B. G., Wei, Y. Y., Brennan, D. L., Fulghum, J. R., Hsiao, H. M., Ma, S., Maxwell, J. P., Cottrell, K. M., Perni, R. B., Gates, C. A., and Kwong, A. D. (2004) *J Biol Chem* **279**, 17508-17514
11. Reesink, H. W., Zeuzem, S., Weegink, C. J., Forestier, N., van Vliet, A., van de Wetering de Rooij, J., McNair, L., Purdy, S., Chu, H.-M., and Jasen, P. L. M. (2005) *In 36th Digestive Disease Week, Chicago, IL, USA*
12. Trozzi, C., Bartholomew, L., Ceccacci, A., Biasiol, G., Pacini, L., Altamura, S., Narjes, F., Muraglia, E., Paonessa, G., Koch, U., De Francesco, R., Steinkuhler, C., and Migliaccio, G. (2003) *J Virol* **77**, 3669-3679
13. Lu, L., Pilot-Matias, T. J., Stewart, K. D., Randolph, J. T., Pithawalla, R., He, W., Huang, P. P., Klein, L. L., Mo, H., and Molla, A. (2004) *Antimicrob Agents Chemother* **48**, 2260-2266
14. Foy, E., Li, K., Wang, C., Sumpter, R., Jr., Ikeda, M., Lemon, S. M., and Gale, M., Jr. (2003) *Science* **300**, 1145-1148
15. Li, K., Foy, E., Ferreon, J. C., Nakamura, M., Ferreon, A. C., Ikeda, M., Ray, S. C., Gale, M., Jr., Lemon, S. M., Wang, C., and Sumpter, R., Jr. (2005) *Proc Natl Acad Sci U S A* **102**, 2992-2997
16. Nakabayashi, H., Taketa, K., Miyano, K., Yamane, T., and Sato, J. (1982) *Cancer Res* **42**, 3858-3863.
17. Yi, M., Bodola, F., and Lemon, S. M. (2002) *Virology* **304**, 197-210
18. Lohmann, V., Korner, F., Koch, J., Herian, U., Theilmann, L., and Bartenschlager, R. (1999) *Science* **285**, 110-113.
19. Blight, K. J., Kolykhalov, A. A., and Rice, C. M. (2000) *Science* **290**, 1972-1974.
20. Bourne, N., Pyles, R. B., Yi, M., Veselenak, R. L., Davis, M. M., and Lemon, S. M. (2005) *Antiviral Res* **67**, 76-82
21. Yi, M., and Lemon, S. M. (2004) *J Virol* **78**, 7904-7915
22. Taremi, S. S., Beyer, B., Maher, M., Yao, N., Prosise, W., Weber, P. C., and Malcolm, B. A. (1998) *Protein Sci* **7**, 2143-2149.
23. Zhang, R., Beyer, B. M., Durkin, J., Ingram, R., Njoroge, F. G., Windsor, W. T., and Malcolm, B. A. (1999) *Anal Biochem* **270**, 268-275.
24. Morrison, J. F., and Walsh, C. T. (1988) *Adv Enzymol Relat Areas Mol Biol* **61**, 201-301
25. Kuzmic, P., Sideris, S., Cregar, L. M., Elrod, K. C., Rice, K. D., and Janc, J. W. (2000) *Anal Biochem* **281**, 62-67
26. Back, S. H., Kim, J. E., Rho, J., Hahm, B., Lee, T. G., Kim, E. E., Cho, J. M., and Jang, S. K. (2000) *Protein Expr Purif* **20**, 196-206
27. Yao, N., Reichert, P., Taremi, S. S., Prosise, W. W., and Weber, P. C. (1999) *Structure Fold Des* **7**, 1353-1363
28. Arasappan, A., Njoroge, F. G., Chan, T. Y., Bennett, F., Bogen, S. L., Chen, K., Gu, H., Hong, L., Jao, E., Liu, Y. T., Lovey, R. G., Parekh, T., Pike, R. E., Pinto, P., Santhanam, B., Venkatraman, S., Vaccaro, H., Wang, H., Yang, X., Zhu, Z., McKittrick, B., Saksena, A. K., Girijavallabhan, V., Pichardo, J., Butkiewicz, N., Ingram, R., Malcolm, B., Prongay, A., Yao, N., Marten, B., Madison, V., Kemp, S., Levy, O., Lim-Wilby, M., Tamura, S., and Ganguly, A. K. (2005) *Bioorg Med Chem Lett* **15**, 4180-4184
29. Krieger, N., Lohmann, V., and Bartenschlager, R. (2001) *J Virol* **75**, 4614-4624.
30. Berger, A., and Schechter, I. (1970) *Philos Trans R Soc Lond B Biol Sci* **257**, 249-264
31. Meylan, E., Curran, J., Hofmann, K., Moradpour, D., Binder, D., Bartenschlager, R. and Tschoopp, J. (2005) *Nature* **437**, 1167-72

32. Li, X., Sun, L., Seth, R.B., Pineda, G. and Chen, Z.J. (2005) *Proc Natl Acad Sci U S A* **102**, 17717–17722
33. Wang, W., Lahser, F. C., Yi, M., Wright-Minogue, J., Xia, E., Weber, P. C., Lemon, S. M., and Malcolm, B. A. (2004) *J Virol* **78**, 700-709
34. Nijhuis, M., Deeks, S., and Boucher, C. (2001) *Curr Opin Infect Dis* **14**, 23-28
35. Croteau, G., Doyon, L., Thibeault, D., McKercher, G., Pilote, L., and Lamarre, D. (1997) *J Virol* **71**, 1089-1096.
36. Mammano, F., Petit, C., and Clavel, F. (1998) *J Virol* **72**, 7632-7637.
37. Maguire, M. F., Guinea, R., Griffin, P., Macmanus, S., Elston, R. C., Wolfram, J., Richards, N., Hanlon, M. H., Porter, D. J., Wrin, T., Parkin, N., Tisdale, M., Furfine, E., Petropoulos, C., Snowden, B. W., and Kleim, J. P. (2002) *J Virol* **76**, 7398-7406

Figure Legends

Figure 1. Colony formation efficiency (CFE) of Con1 replicon RNAs bearing resistance mutations. Replicon RNAs were transfected into Huh7 cells followed by selection with 500 mg/ml G418 for 2-3 weeks until cell colonies were established. Bars represent the number of replicon colonies/ μ g input RNA; the numbers above each bar show the efficiency normalized to the wild-type (wt) replicon.

Figure 2. Transient replication profile of HCV-N replicons that express the HIV tat protein, inducing SEAP secretion in transfected En5-3 cells. Shown are the SEAP activities present in supernatant culture fluids over four successive days following electroporation of cells with the parental wt replicon, mutated RNAs containing the following SCH6 resistance mutations: A156T, R109K, A156T+P89L, and A156+G162R; and a replication-lethal mutant with a mutation in the active site of the NS5B polymerase, Δ GDD. In this system, SEAP activities closely parallel the abundance of intracellular RNA (17). For each mutant, the data represent the SEAP expression at each time point as a percent of that of the Δ GDD control replicon at 24 hrs after transfection. The data shown are means from two independent experiments.

Figure 3. Wild-type and mutant NS3/4A proteases resistant to SCH6 disrupt Sendai virus infection-induced activation of the ISG56 promoter. Cells were transfected with vectors expressing the wild-type HCV-N NS3-4A segment, with or without the indicated resistance mutations. As a control, cells were transfected in parallel with a vector expressing an active-site NS3 mutant lacking protease activity (S138AA) or with empty vector. Cells were transfected subsequently with an ISG56 promoter luciferase reporter construct, then infected with Sendai virus. The ISG56 promoter stimulation index shown represents the ratio of luciferase activity present in Sendai-infected vs. mock-infected cells, \pm S.E.M. The results show that expression of the wild-type protease or proteases containing the A156T or R109K resistance mutations, but not the active-site S138AA mutant, block virus-induced activation of the ISG56 promoter through the IRF-3 pathway (14,15,31,32).

Figure 4. SCH6 resistance mutations result in impaired *cis* auto-proteolysis of NS3-4A *in vitro*. (A) Auto-proteolysis of an *in vitro* NS3-4A translation product results in the mature NS3/4A protease. (B) SDS-PAGE of [³⁵S]-labeled products of *in vitro* translation reactions programmed with RNA encoding the NS3-4A segment of HCV-N and related SCH6 primary resistance and second-site mutations. Reactions were terminated after 20, 30, and 180 min. wt = wild-type, S138AA = S138A+S139A, an enzymatically inactive NS3 protease mutant. See text for other details. (C) PhosphoImager quantitation of the percent of the translation products shown in panel B that have undergone scission. See panel B for key to symbols.

Figure 5. SCH6 resistance mutations result in impaired *trans*-processing of the NS4B-5A polyprotein segment *in vitro*. (A) Proteolysis of an [³⁵S]-labeled *in vitro* NS4B-5A translation product by an unlabeled, mature NS3/4A protease results in NS4B and NS5A. (B) SDS-PAGE of products of an *in vitro* cleavage reaction containing [³⁵S]-labeled translation reactions programmed with RNA encoding the NS4B-5A segment of HCV-N, to which unlabeled mature NS3/4A protease, both wt and related SCH6 primary resistance and second-site mutations, were added. Cleavage reactions were terminated at the times shown. wt = wild-type. See text for other details. (C) PhosphoImager quantitation of the percent of the labeled NS4B-5A translation products shown in panel B that have undergone scission. See panel B for key to symbols.

Figure 6. Primary SCH6 resistance mutations result in impaired *trans*-processing of the polyprotein in replicon cells. Shown is the result of an immunoblot using antibody directed against NS5A, demonstrating delayed polyprotein processing in replicon cells bearing resistance mutations. The positions of NS5A and the usually non-detectable processing intermediate (p110) are indicated. Lane 1,

normal Huh7 cells; lane 2, wt Con1 replicon cells; lanes 3-7, cells containing replicons with primary SCH6 resistance mutations and the compensatory second-site Q86R mutation.

Figure 7. Two views of the three-dimensional structure of NS3 protease-SCH6 complex. The structure of the SCH6 inhibitor is presented as a stick model. Side chains of key residues are depicted using CPK models on the Connolly surface of the NS3 protease. Colors: *White*, NS34a protease domain; *Dark Blue*, K136, *Light Blue*, R109; *Maroon*, G162; *Orange*, D168; *Green*, A156; *Red*, S139; *Purple*, Q86; *Yellow*, P89. The inhibitor is shown in yellow. Panel **(B)** is a rotation of the protease domain in Panel **(A)** about the Y axis.

Table 1. Genotype 1b Subgenomic HCV Replicon Cell Lines and Compounds

Cell Line	HCV Strain	SCH6 IC ₉₀	SCH6 CC ₅₀
2H8 1.3	Con1	0.4±0.2 μM (n=8)	>10 μM
Ntat2ANeo/EG	HCV-N	1.4±0.01 μM (n=6)	>20 μM

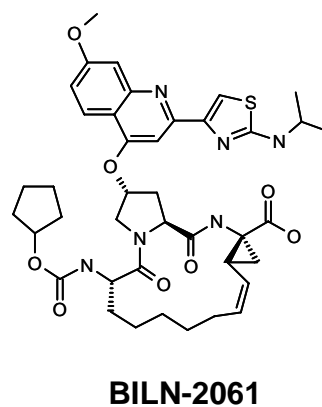
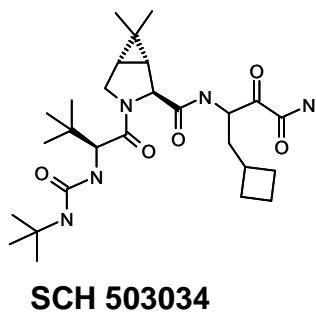
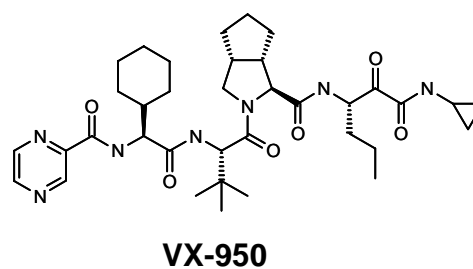
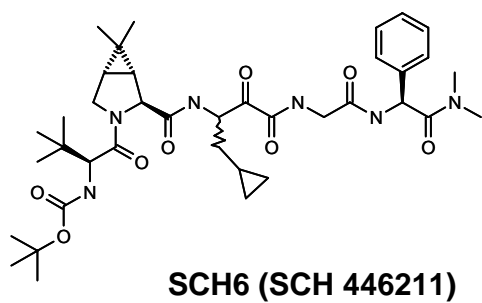


Table 2. NS3 Protease Domain Mutations Associated with SCH6 Resistance.

Mutation	SCH6 Resistant Colonies		cDNA Clones
	2H8 1.3	Ntat2ANeo/EG	2H8 1.3
R109K	0	2	0
A156T	0	1	4
R109K+A156V	0	0	1
I153V	0	0	1
R109K+I153V	2	0	1
Total	2	3	7

Table 3. Impact of NS3 Mutations on Protease Activity and Replicon Resistance to SCH6.

Mutation	Cell-Free Protease Assay			Replicon Cells SCH6 IC ₉₀ (μM)	
	K _m (μM)	K _{cat} (min ⁻¹)	SCH6 K _i * (nM) ¹	Con1	HCV-N
<i>Wild-type Protease</i> ²					
None	5±1 ³ (n=4)	25±6	7±4 (n=8)	0.4±0.2 (n=8)	1.4±0.01 (n=6)
<i>Mutations Selected by Passage of Replicon Cells in SCH6</i>					
R109K	10±1 (n=2)	15±1	45±30 (n=2)	1.2±0.3 (n=2)	3.2±0.36 (n=2)
A156T	26±4 (n=3)	17±7	130±30 (n=6)	7.0±3.0 (n=3)	20±0.01 (n=3)
R109K+A156T	38±3 (n=2)	15±1	1500 (n=1)	>40	ND ⁴
I153V	4 (n=1)	8	19±1 (n=3)	0.28±0.02 (n=2)	ND
R109K+I153V	3 (n=2)	3±0.5	22±2 (n=2)	1.4±0.2 (n=2)	ND
<i>Second-Site Compensatory Mutations</i>					
A156T+G162R	ND	ND	ND	ND ⁴	17±2.7 (n=3)
A156T+P89L	ND	ND	ND	ND	16±1.5 (n=3)
A156T+Q86R	37±4 (n=4)	5±2	79±8 (n=2)	1.9 (n=1)	ND
Q86R	6±1 (n=4)	14±2	2.5±0.7 (n=2)	0.08 (n=1)	ND

¹See Materials and Methods for definition of the inhibition constant, *K_i.

²HCV-BK strain single-chain NS3 protease (22).

³Values ± standard deviation or range.

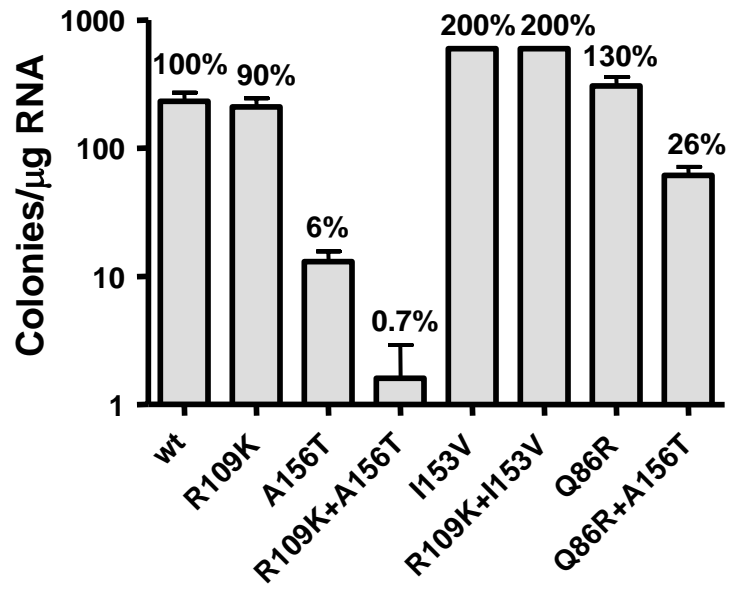
⁴ND = not done; mutations were studied only in the HCV replicon background in which selected.

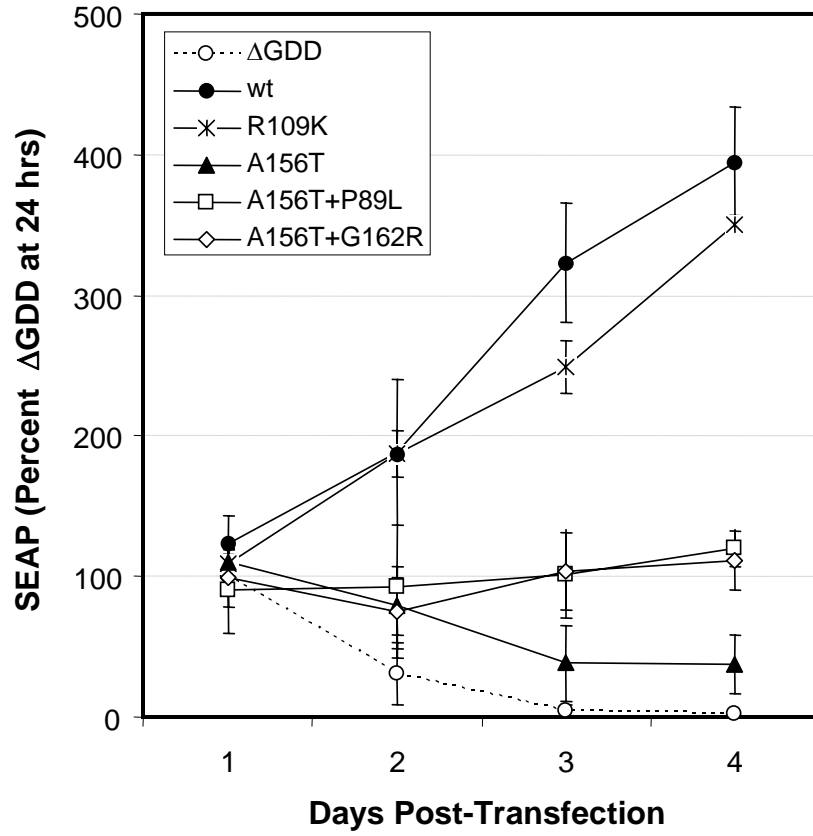
Table 4. Potency of inhibitors against wild-type protease and protease containing resistance mutations.

Mutation	Inhibition Constant (nM) ¹			
	SCH6 ²	SCH 503034	BILN 2061	VX-950
Wild-type	7	30	0.8	30
R109K	45	45	0.3	55
A156T	130	8300	900	13000
I153V	19	19	0.7	24
D168V	4	20	190	12

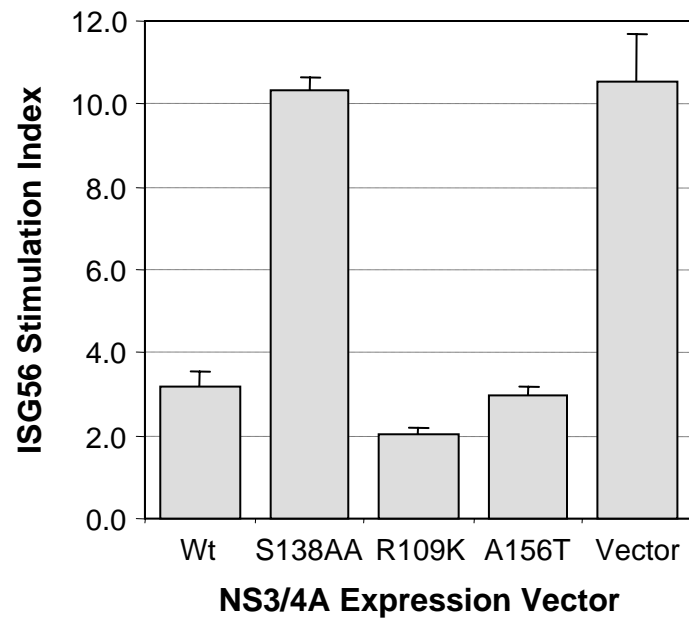
¹See Materials and Methods for definition of K_i^* (calculated for SCH6, SCH 503034, and VX-950) and the tight-binding inhibition constant, K_i ; (calculated for BILN 2061). The 95% confidence interval for the K_i^* determinations was 2-fold.

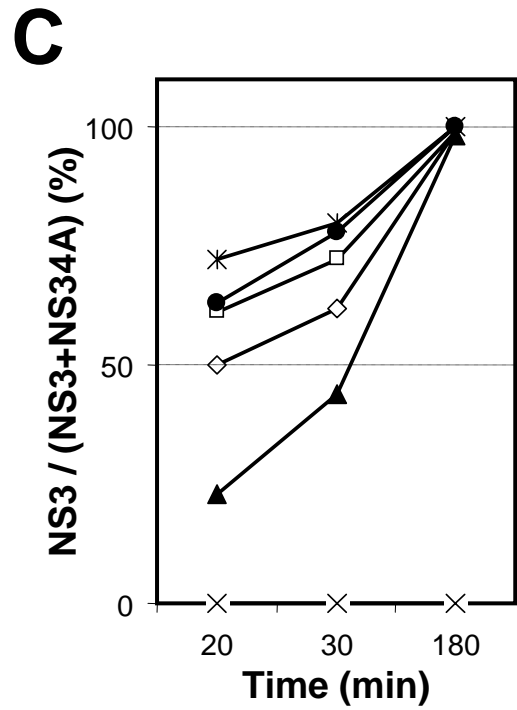
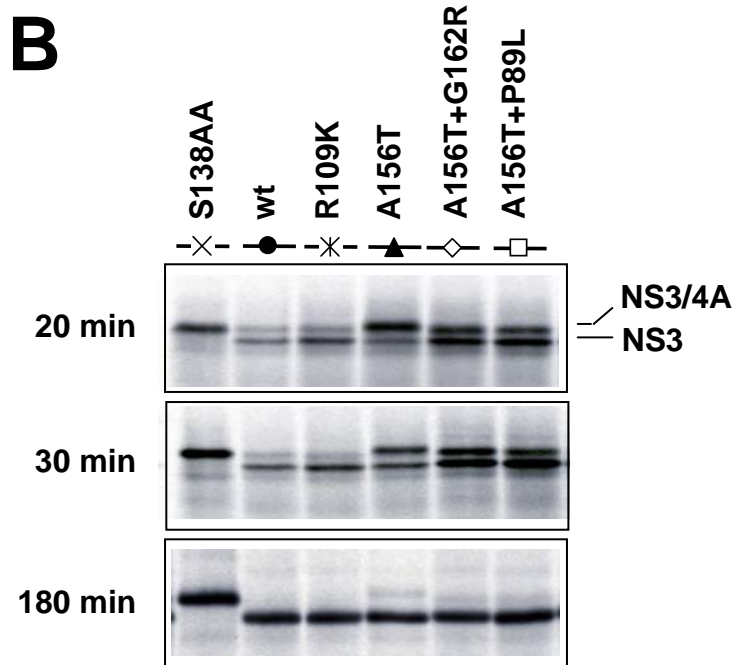
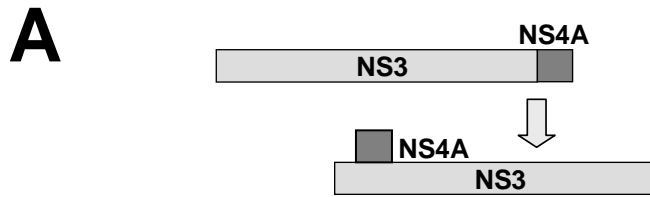
²SCH6 data are taken from Table 3.

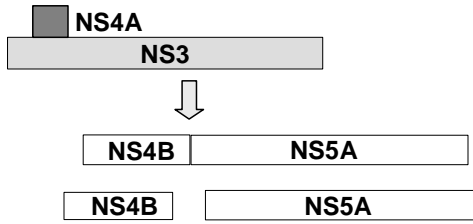
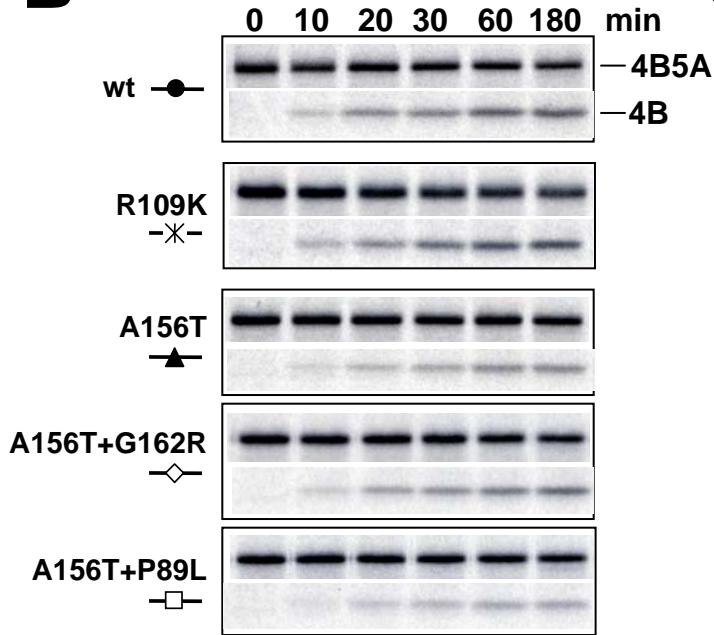




Yi et al., Figure 2





A**B****C**